Measurement of Aerodynamic Passive Twisting in Lattice-Structured Propeller Blades via Wind Tunnel Tests

Ju-Hoe Kim[1], Yuta Nishijima[2], Yuta Yaguchi[3] and Takeshi Tsuchiya[1]

[1] Department of Aeronautics and Astronautics, The University of Tokyo, Tokyo, Japan
[2] Department of Aerospace Engineering, National Defense Academy, Yokosuka, Japan
[3-]Division of Creative Activity, The University of Tokyo, Tokyo, Japan

Abstract. This research proposes a new passive variable pitch propeller with a lattice structure. Introducing the lattice structure gives a propeller a characteristic that makes it easier to deform in a specific direction. In the proposed propeller, a quasi-cube lattice modified to fit an airfoil shape is used to give the propeller a torsional deformable characteristic, and the goal is to realize a variable pitch mechanism without using a mechanical device. A prototype propeller was created using a 3D printer and evaluated in a torsion test and wind tunnel. Torsion tests revealed that the surface film strengthens the torsional rigidity of the proposed propeller. These results suggest that the film's effect should be considered when designing more sophisticated lattice propellers. Wind tunnel tests confirmed that the prototype propeller was de-formed but not destroyed, and the propeller generated thrust. A high-speed camera photographed the deformation of the propeller and it was observed that the deformation was composed of bending and torsion. The observed maximum torsional angle was about 3 degrees. These results suggest the feasibility of the proposed concept.

Keywords: Unmanned Aerial Vehicle, Propeller, Morphing Wing, Additive Manufacturing, Lattice Structure.

1 Introduction

1.1 Passive Variable Pitch Propeller

In recent years, electric unmanned aerial vehicles (UAVs) have become widely used in the civilian sector and are expected to be applied to large-scale aerial photography and logistics. Electric UAVs come in various forms, including multi-copters, fixed-wing and hybrid types. However, most of them use propellers to generate thrust, so improving propeller performance impacts them. Several propeller design methods have been devised to meet the performance requirements for a given cruise condition, but there is a performance trade-off between the cruise condition and others. Variable pitch propellers improve the propeller performance trade-off that changes the propeller's pitch according to the flight conditions. These propellers have been put to practical use in UAV-scale propellers by using servomotors to control a mechanical mechanism installed on

the propeller blades. In previous research, a propeller can always maintain the optimum pitch angle during flight by passive pitch change using aerodynamic forces during flight without electronic control [1]. This propeller has been devised by designing the propeller in consideration of aerodynamic twisting moment. However, a mechanical variable system is still required for that pitch control system.

1.2 Lattice Structure

A new structural approach to passive propeller blade pitch variation is investigated. A lattice-structured wing is known as a form of morphing wing [2]. This type of morphing wing can be designed to accept user-defined deformations. This research proposes a twisting acceptable lattice-structured propeller to realize a passive variable pitch propeller without mechanical structure such as gears and hinges. There are many possibilities for the specific shape of the lattice structure. This study uses a modified version of the cube lattice to fit the wing shape. Cube lattices have been reported to be flexible in the torsional direction by Nishijima eta al [2]. The proposed propeller is evaluated experimentally through wind tunnel tests.

2 Sample Manufacturing and Torsion Tests

2.1 Lattice-Structured Propeller Design

The prototype propeller was a simple rectangular blade shape to facilitate 3D printing. The diameter is 250 mm and the chord length is 30 mm. The airfoil shape is the Eppler 325 [3]. The blade angle is 20 degrees and uniform in the span direction. Figure 1 shows a 3D model of the prototype lattice-structured propeller.

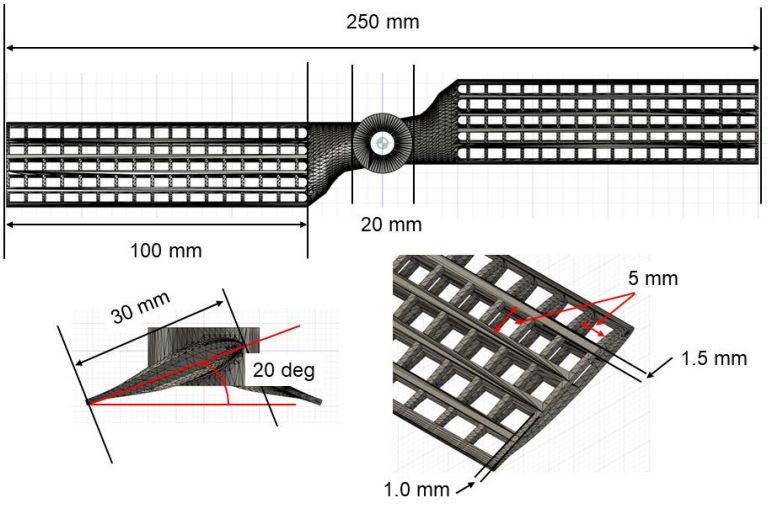

Fig. 1. 3D model of prototype lattice structured propeller

2.2 Propeller Manufacturing

Sample propellers for wind tunnel tests and torsion tests were manufactured by a SLS type 3d printer [4]. The material of propellers was Nylon 12 powder [5]. The propeller surface was made by attaching a polyester film. This film is commonly used in radio-controlled aircraft [6]. Propellers with film applied were checked for center-of-gravity balance and adjusted by applying tape. Figures 2 and 3 show manufactured propellers and an overview of balance checking.

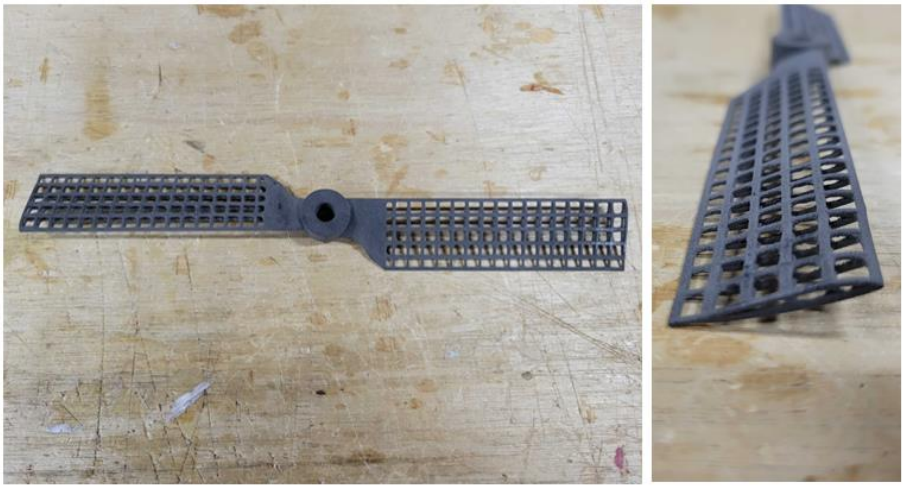

Fig. 2. Manufactured propeller

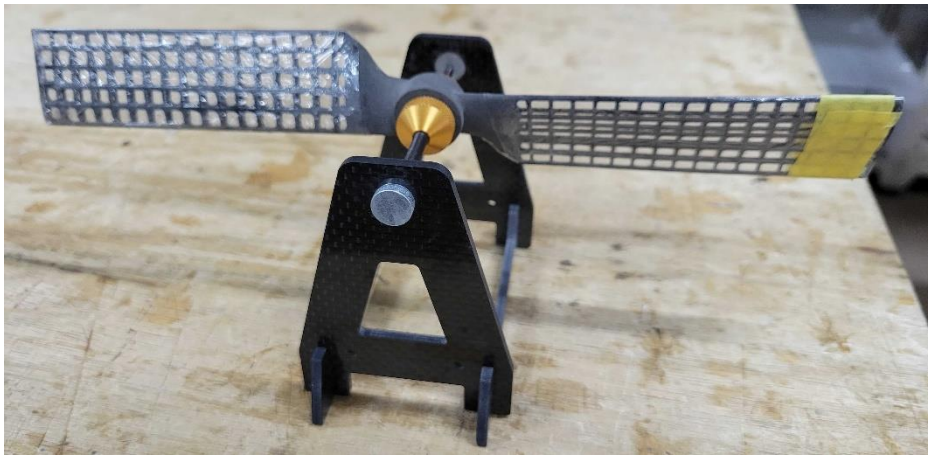

Fig. 3. Overview of balance checking

2.3 Torsion Tests

Figure 4 shows an illustrated outline of torsion tests. A metal rod was inserted into the center of the propeller hub, and a tensile load was applied to the metal rod via a thread and pulley. The displacement of the rod was measured with a laser displacement meter [7], and the twist angle of the propeller was calculated. The tensile load was controlled by adjusting the amount of a 10 g weight. Two tests are conducted for the propeller with film applied and the propeller without film. Figure 5 shows an overview of torsion tests. Nishijima et al. has shown that rectangle wing structures constructed with cube lattice exhibit a nearly linear twist angle distribution concerning the concentrated torsional moment in the span direction [2]. This result was assumed to hold for the sample propeller.

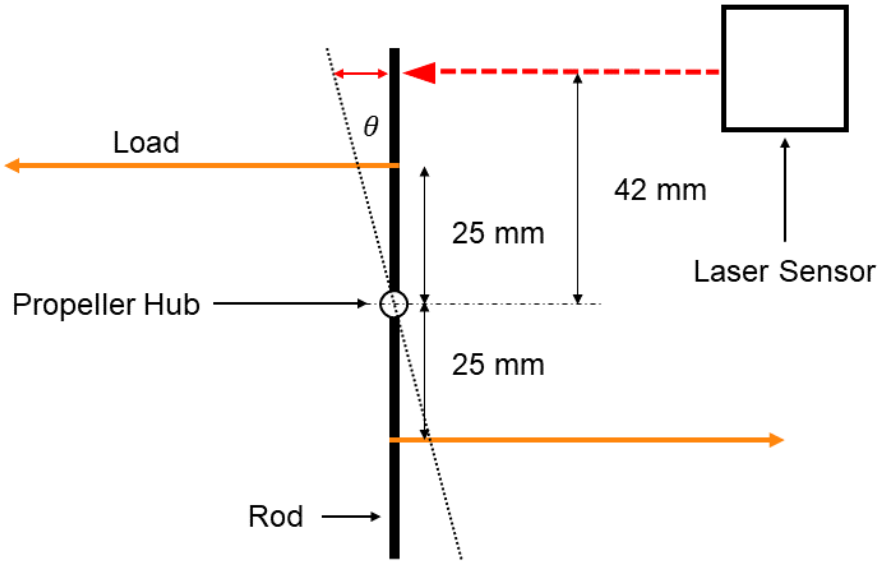

Fig. 4. Illustrated outline of torsion tests

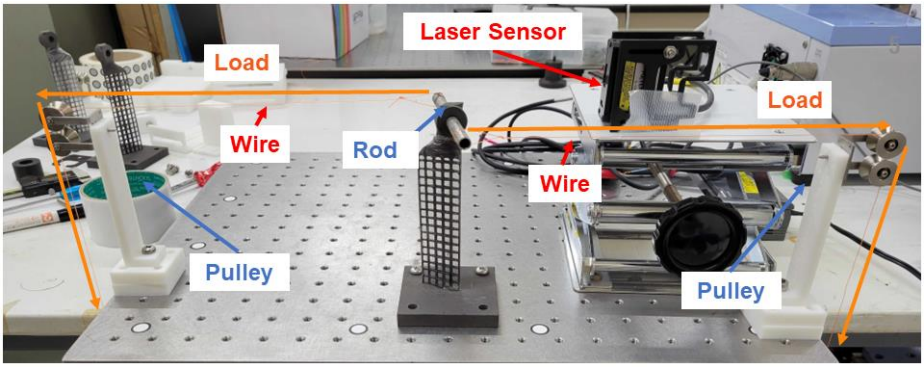

Fig. 5. Overview of torsion tests

Figure 6 shows the results of the torsion tests. The positive direction of the torsional moment and torsional angle is the direction in which the blade's leading edge is raised.

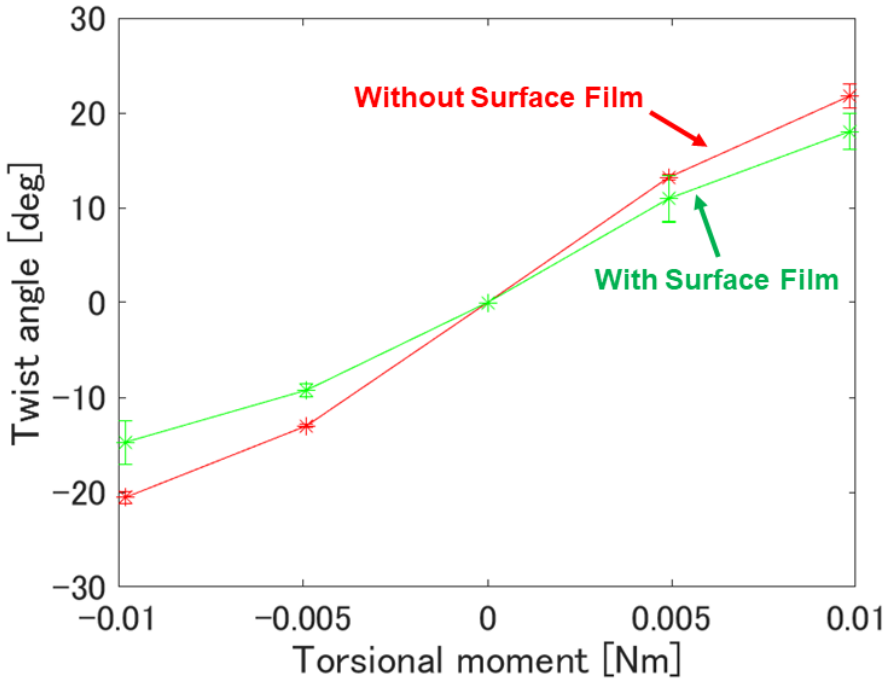

Fig. 6. Results of torsion tests

Results of torsion tests show that the torsional rigidity of lattice structured propeller is enforced when the wing has a surface film.

3 Wind Tunnel Tests

3.1 Setting of Wind Tunnel Tests

Figure 7 shows an illustrated outline of wind tunnel tests. The used wind tunnel is a low-speed wind tunnel at the University of Tokyo. The upper wind speed limit of this wind tunnel is 15 m/s. A six-axis force sensor [8] was used to measure the thrust and torque generated by the propeller. Propeller's rotational speed is measured by a tachometer [9]. A high-speed camera [10] was used to visualize propeller deformation.
Figure 8 shows an overview of wind tunnel tests. The reason why the wires are not tight is to prevent thrust from acting on the wires.

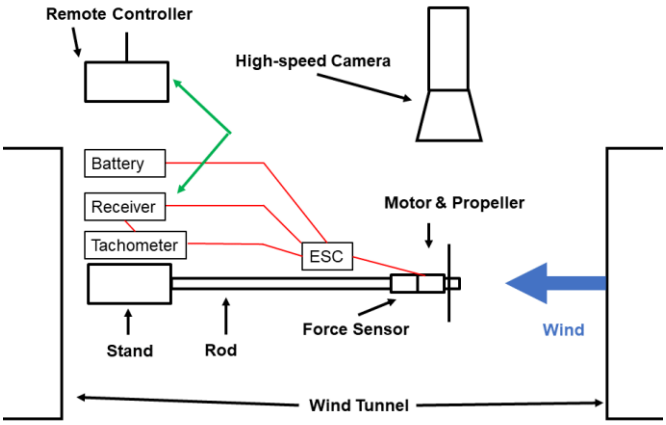

Fig. 7. Illustrated outline of wind tunnel tests

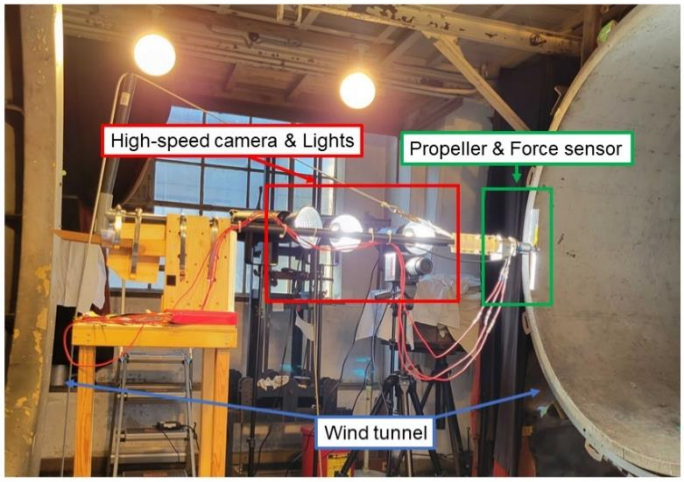

Fig. 8. Overview of wind tunnel tests

Figures 9 to 11 show the validation results of the wind tunnel test setup. Wind tunnel test data published by the University of Illinois [11] were used as validation data. The used propeller was APC 10x7E and rotational speed was 5000 RPM. The horizontal axis in each figure is advance ratio J defined by equation xx. Thrust coefficient C_T, Power coefficient C_P and Propeller efficiency η is calculated from equations 1 to 6. The power consumed by the propeller is calculated from Equation x using the torque measured by the force sensor and the propeller's rotational speed Ω [rpm] measured by the tachometer. The plot shows the average value during the measurement time, and the error bars show time variability up to 2 sigma.

$$J = \frac{U}{nD} \quad [1]$$

$$C_{\mathrm{T}} = \frac{T}{\rho n^2 D^4} \quad [2]$$

$$C_{\mathrm{P}} = \frac{P}{\rho n^3 D^5} \quad [3]$$

$$\eta = J\frac{C_{\mathrm{T}}}{C_{\mathrm{P}}} \quad [4]$$

$$P = \Omega Q \quad [5]$$

$$\Omega = 2\pi n \quad [6]$$

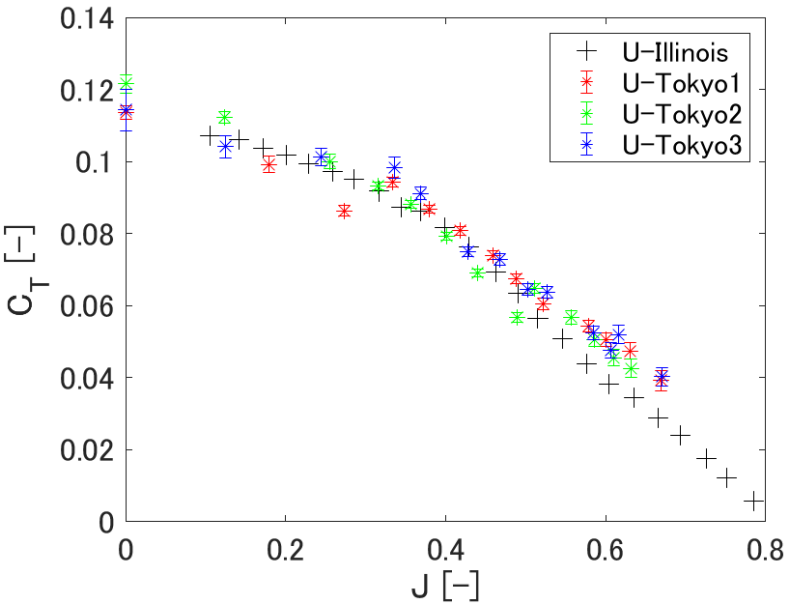

Fig. 9. Validation of measurements: Thrust

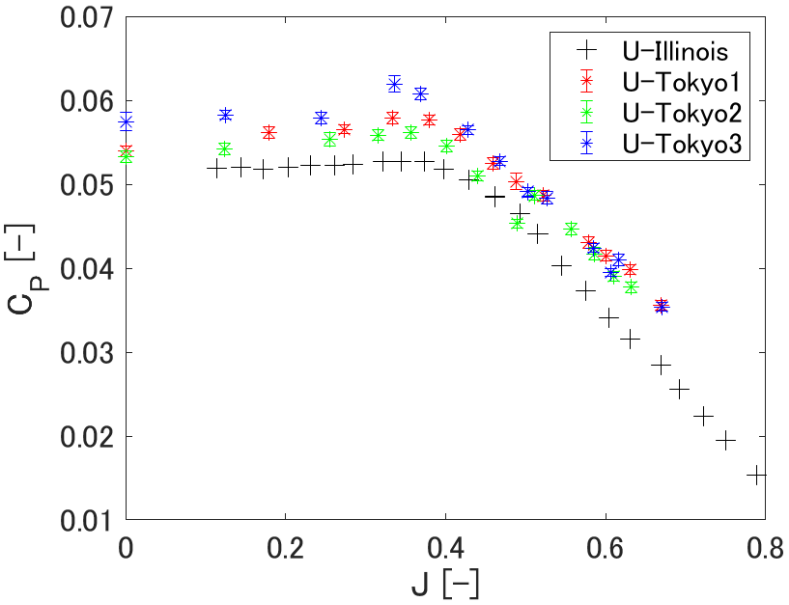

Fig. 10. Validation of measurements: Power

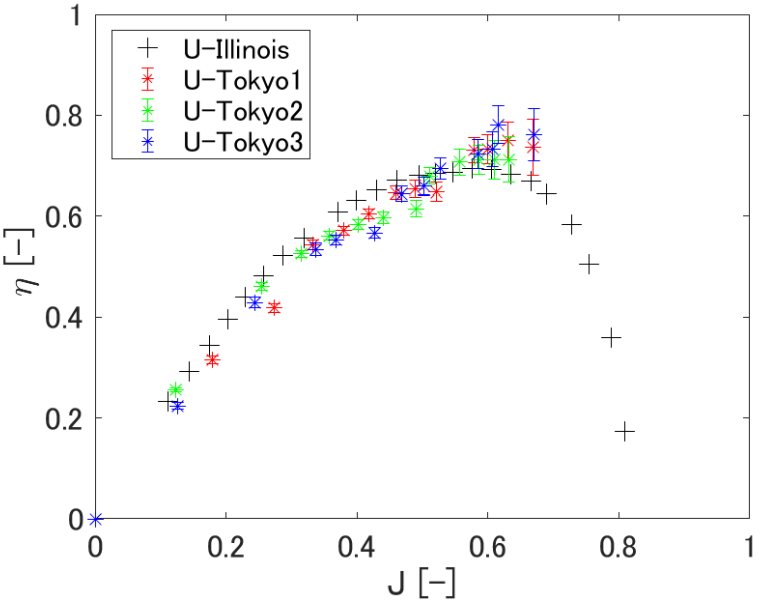

Fig. 11. Validation of measurements: Efficiency

3.2 Propeller Performance Measurement

Two wind tunnel tests were conducted for each propeller operating condition because the propeller film peeled off during the first test. Figure 12 shows an example of film peeling. An instant glue was used to hold the film during the second test. Figures 13 to 18 show the results of wind tunnel tests. The prototype lattice-structured propeller generates thrust and the thrust and power consumption increase with increasing rotational speed. The efficiency of a conventional propeller improves with rotational speed at the same advance ratio as the lift coefficient increases due to the 3D flow effects [12], but the prototype propeller exhibited behavior that did not follow the trends. This unconventional behavior may depend on the deformation of the propeller.
The surface film easily affects propeller performance and needs to improve reproducibility of film application.

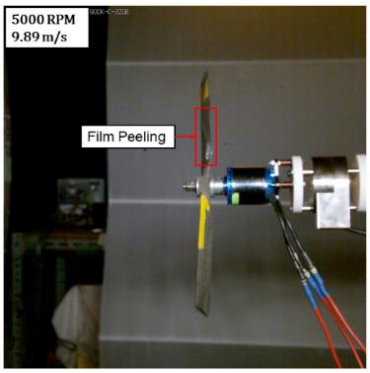

Fig. 12. Example of film peeling

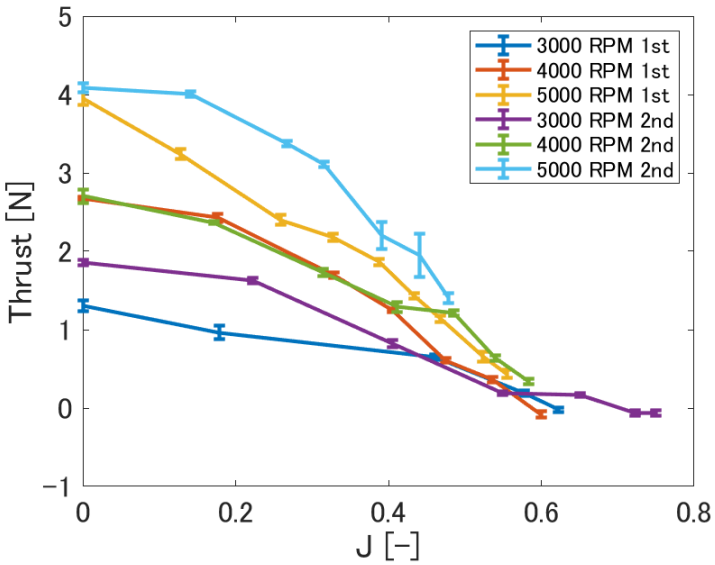

Fig. 13. Propeller Performance: Thrust

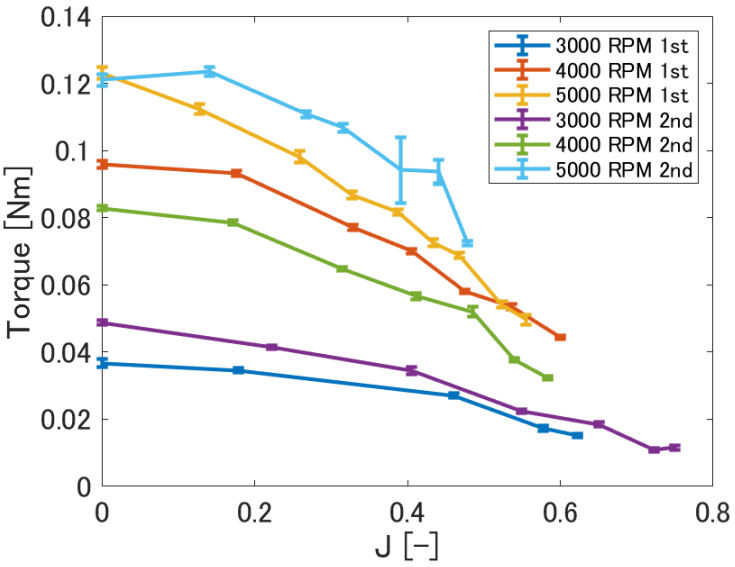

Fig. 14. Propeller Performance: Torque

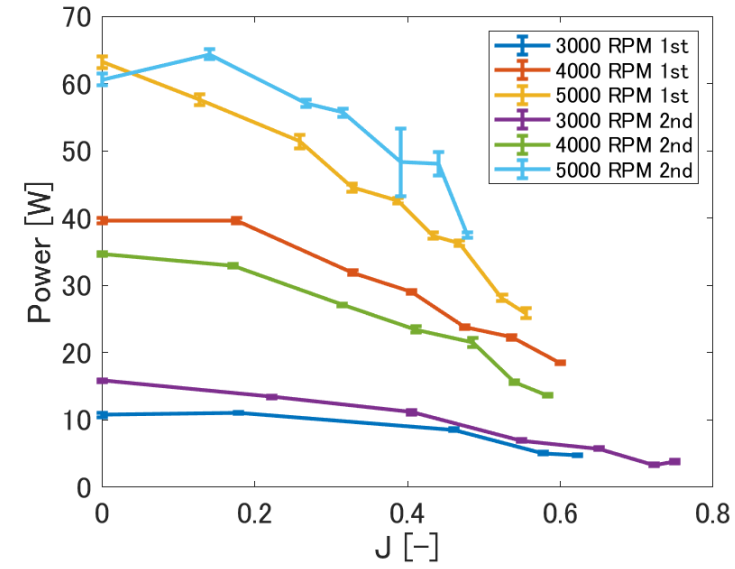

Fig. 15. Propeller Performance: Power

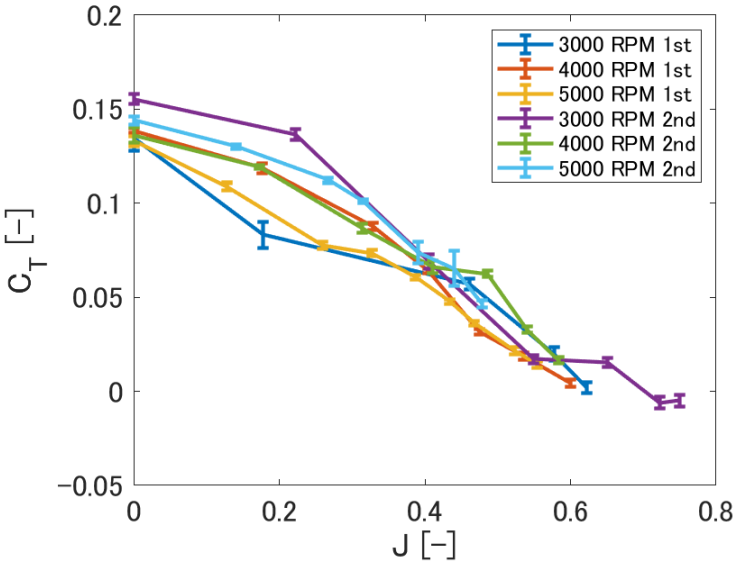

Fig. 16. Propeller Performance: Thrust coefficient

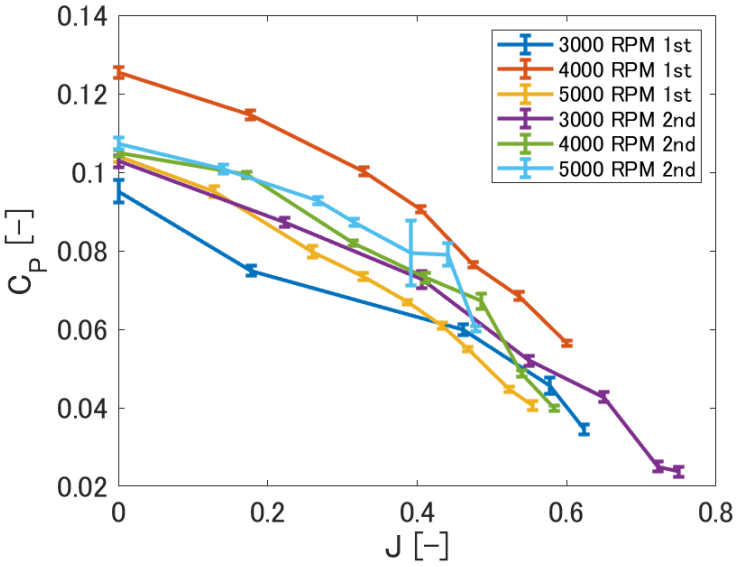

Fig. 17. Propeller Performance Power coefficient

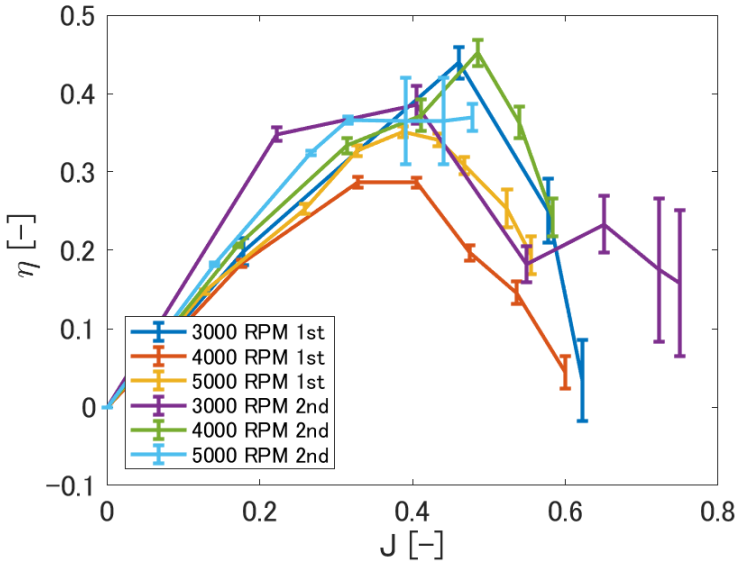

Fig. 18. Propeller Performance: Efficiency

3.3 Shooting with a High-Speed Camera

A high-speed camera shot the behavior of the propeller during the second time wind tunnel test. The frame rate for shooting was 6200 fps. The propeller exhibits a mixture of bending and torsional deformation. As a quantitative measure of deformation, the relative bending angle $\theta_{b,t}$ and twist angle $\theta_{t,r}$ is used. Each angle is defined as following equations.

$$\theta_{b,r} = \theta_{b,i} - \theta_{b,0} \quad [7]$$

$$\theta_{t,r} = \theta_{t,i} - \theta_{t,0} \quad [8]$$

$\theta_{b,0}$ and $\theta_{t,0}$ are the angles that the propeller blade makes with the reference position at 0 rotational speed and 0 wind speed. $\theta_{b,i}$ and $\theta_{t,r}$ are the angles from the reference position that depend on the propeller operating conditions. Overviews of angle definitions are shown in Figure 19. Each angle was measured from images taken by a high-speed camera, and ImageJ [13] was used as the measurement software. The result of the measurement was that $\theta_{b,0}$ was 18 degrees and $\theta_{t,0}$ was 89 degrees. The angular change of 1 to 2 degrees from the designed shape is considered to be due to the heat applied when the surface film is attached and the film's tension. Table 1 shows the results of angle measurements. The prototype propeller was torsional deformed in the direction of decreasing pitch, but the angle was only about 3 degrees at most.

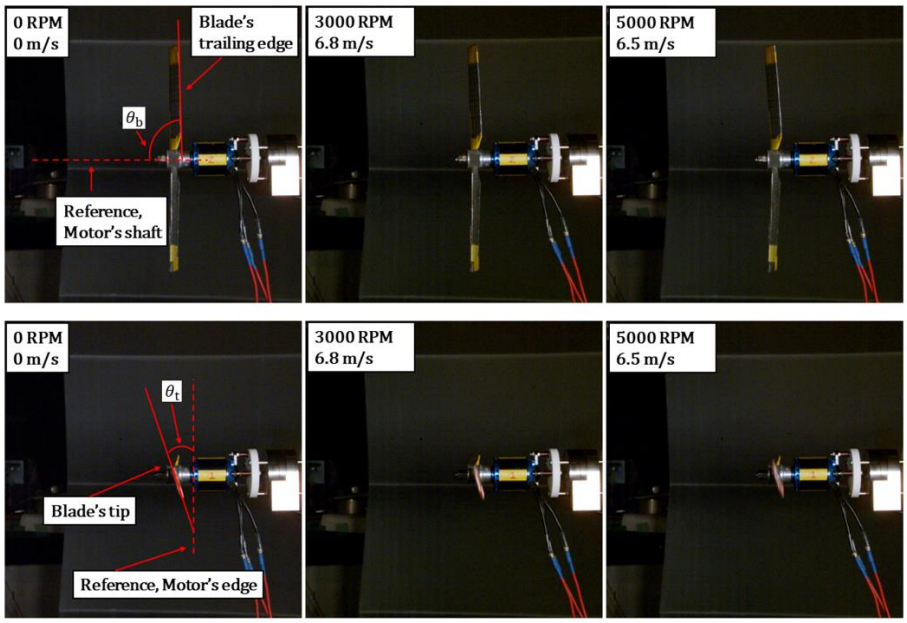

Fig. 19. Overview of angle definitions

Table 1. Results of angle measurements

RPM	Wind Velocity [m/s]	$\theta_{b,r}$ [deg]	$\theta_{t,r}$ [deg]
0	0	0	0
3000	0	-3.5	-2.8
3000	2.9	-4.3	-2.1
3000	6.8	-2.2	-2.7
3000	8.9	-1.1	-3.4
4000	0	-3.8	-1.2
4000	3.3	-2.9	-2.2
4000	6.8	-2.7	-2.7
4000	8.9	-2.4	-1.9
5000	0	-3.9	-0.6
5000	3	-3.4	-1.2
5000	6.5	-3.5	-2
5000	9	-2.7	-0.8

4 Conclusions

As a new efficient propeller for UAVs, a passive variable pitch propeller with reduced mechanical elements was proposed by introducing a lattice structure and a prototype was manufactured. Torsional tests were conducted on lattice-structured propellers, and it was confirmed that a surface film increased the torsional rigidity. Wind tunnel tests confirmed that the prototype propeller was deformed but not destroyed, and the propeller generated thrust. A high-speed camera shot the deformation of the propeller and it was observed that the deformation was composed of bending and torsion. The observed maximum torsional angle was about 3 degrees. These results suggest the feasibility of the proposed concept. Reducing the negative effects on repeatability that occur when applying the film and measuring propeller deformation more precisely are future issues.

Acknowledgments

The authors thank Professor Hiroaki Tanaka and Yusuke Arai, who belong to National Defense Academy of Japan, for supporting torsion tests. We also thank Ryohei Kojima, Yusuke Hayashi and Akihiro Arimoto, who belong to Tsuchiya laboratory at the University of Tokyo for supporting wind tunnel tests. Dr Hiroki Igarashi who belongs to the University of Tokyo provides authors with a high-speed camera. Without Dr. Hiroki's support, this research would not have been possible. This work is supported by JST SPRING, Grant Number JPMJSP2108.

References

1. Heinzen, S. B., Hall, C. E. Jr., and Gopalarathnam, A.: Development and Testing of a Passive Variable-Pitch Propeller, JOURNAL OF AIRCRAFT, Vol. 52, No.3, May-June 2015
2. Nishijima, Y., Tanaka, H., Biron, A., and Miura, Takashi.: Variations in Structural Properties of Lattice Structures Depending on Unit Cell Shape for Morphing Wings, Proceedings of the 33rd congress of the international council of the aeronautical sciences, ICAS2022, Stockholm, https://www.icas.org/ICAS_ARCHIVE/ICAS2022/index.htm
3. Airfoil tools, http://airfoiltools.com/airfoil/details?airfoil=e325-il, last accessed 2023/07/31.
4. Formlabs Homepage, https://formlabs.com/3d-printers/fuse-1/, last accessed 2023/07/31.
5. Formlabs Homepage, https://support.formlabs.com/s/article/Using-Nylon-12?language=en_US, last accessed 2023/07/31.
6. OK MODEL Homepage, https://www.okmodel.co.jp/catalog_accessories/25033/, last accessed 2023/07/31.
7. Keyence Homepage, https://www.keyence.co.jp/products/sensor/positioning/il/models/il-100/, last accessed 2023/07/31.
8. Leptrino Homepage, https://www.leptrino.co.jp/product/6axis-force-sensor, last accessed 2023/07/31.
9. FUTABA Homepage, https://www.rc.futaba.co.jp/products/detail/I00000111, last accessed 2023/07/31.
10. Photron Homepage,

https://www.photron.co.jp/products/hsvcam/fastcam/fa-mini-feature.html,
last accessed 2023/07/31.
11. Brandt, J.B.: Small-Scale Propeller Performance at Low Speeds, Master's Thesis, 2005, University of Illinois at Urbana-Champaign, Urbana, Illinois, US.
12. Snel, H., Houwink, R. and Bosschers, J.: Sectional prediction of lift coefficients on rotating wind turbine blades in stall, Tech Rep ECN-C–93-052, December 1994, National Aerospace Laboratory (NLR), Netherlands.
13. ImageJ Homepage, https://imagej.nih.gov/ij/download.html, last accessed 2023/07/31.